

A ventricular-vascular coupling model in presence of aortic stenosis

Damien Garcia,¹ Paul J. C. Barenbrug,² Philippe Pibarot,³ André L. A. J. Dekker,² Frederik H. van der Veen,² Jos G. Maessen,² Jean G. Dumesnil,³ and Louis-Gilles Durand¹

¹Clinical Research Institute of Montreal, Montreal, Quebec, Canada; ²Department of Cardiothoracic Surgery, Academic Hospital, Maastricht, The Netherlands; and ³Quebec Heart Institute, Laval Hospital, Laval University, Quebec, Canada

Submitted 27 July 2004; accepted in final form 8 December 2004

Garcia, Damien, Paul J. C. Barenbrug, Philippe Pibarot, André L. A. J. Dekker, Frederik H. van der Veen, Jos G. Maessen, Jean G. Dumesnil, and Louis-Gilles Durand. A ventricular-vascular coupling model in presence of aortic stenosis. *Am J Physiol Heart Circ Physiol* 288: H1874–H1884, 2005. First published December 16, 2004; doi:10.1152/ajpheart.00754.2004.—In patients with aortic stenosis, the left ventricular afterload is determined by the degree of valvular obstruction and the systemic arterial system. We developed an explicit mathematical model formulated with a limited number of independent parameters that describes the interaction among the left ventricle, an aortic stenosis, and the arterial system. This ventricular-valvular-vascular (V^3) model consists of the combination of the time-varying elastance model for the left ventricle, the instantaneous transvalvular pressure-flow relationship for the aortic valve, and the three-element windkessel representation of the vascular system. The objective of this study was to validate the V^3 model by using pressure-volume loop data obtained in six patients with severe aortic stenosis before and after aortic valve replacement. There was very good agreement between the estimated and the measured left ventricular and aortic pressure waveforms. The total relative error between estimated and measured pressures was on average (standard deviation) 7.5% (SD 2.3) and the equation of the corresponding regression line was $y = 0.99x - 2.36$ with a coefficient of determination $r^2 = 0.98$. There was also very good agreement between estimated and measured stroke volumes ($y = 1.03x + 2.2$, $r^2 = 0.96$, SEE = 2.8 ml). Hence, this mathematical V^3 model can be used to describe the hemodynamic interaction among the left ventricle, the aortic valve, and the systemic arterial system.

mathematical modeling; cardiovascular system; cardiac catheterization; left ventricle

LEFT VENTRICULAR (LV) pressure, aortic pressure, and cardiac output result from a matching among the oxygen demand of the body, the LV performance, and the LV afterload. The presence of an aortic valve stenosis causes an obstruction to LV outflow, thus resulting in an increase in LV afterload (20). Patients with aortic stenosis also often have concomitant diseases, including hypertension, hyperlipidemia, diabetes, and atherosclerosis (1, 6, 22, 25). These diseases have been shown to alter the structural and functional properties of the systemic arterial system (8, 40). More specifically, they may reduce arterial elasticity and/or increase arteriolar resistance. Hence in patients with aortic stenosis, the left ventricle is often facing a double load: a valvular load imposed by the aortic stenosis and an arterial load caused by a decrease in systemic arterial compliance (C) and/or an increase in systemic vascular resistance (R). Briand et al. (3) have recently shown that reduced C is a frequent occurrence in patients with aortic stenosis where

it independently contributes to increase afterload and decrease LV function. In addition, Antonini-Canterin et al. (1) have reported that symptoms of aortic stenosis develop at a lesser degree of valvular obstruction in hypertensive compared with normotensive patients. It is thus important to assess the respective contributions of the aortic valve and the systemic arterial system to the LV workload in such patients. This information could be useful to preferentially target the treatment on the valve (i.e., valve replacement), on the systemic arterial system (i.e., medical therapy), or on both, given the type and magnitude of afterload augmentation. We thus developed a mathematical ventricular-valvular-vascular model (V^3 model) to study the coupled system formed by the left ventricle, a normal or stenotic aortic valve, and the systemic arterial system. A simple mathematical model describing the interaction between the left ventricle and the arterial system has been recently proposed by Segers et al. (26–28) and has been proven to correctly predict some clinical observations. We (13) completed the model of Segers with a newly validated equation describing the instantaneous transvalvular pressure-flow relationship. The objective of the present study was to assess the descriptive validity of the resulting V^3 model using catheterization data obtained in six patients immediately before and after aortic valve replacement (9).

MATERIALS AND METHODS

Analytic model. Transvalvular flow rate was simulated using the V^3 model (Fig. 1). The latter consists on the interaction among 1) the time-varying elastance model for the left ventricle (35), 2) the instantaneous net pressure gradient across the aortic valve (13), and 3) the three-element windkessel model for the systemic arterial load (38). The LV time-varying elastance (E) model relates the ventricular pressure (P_V) to the ventricular volume (V) and the unloaded volume, defined as the intercept of the end-systolic pressure-volume relationship with the volume axis (V_0) (35) as follows:

$$E(t) = \frac{P_V(t)}{V(t) - V_0} \quad (1)$$

With regard to the aortic valve, we (13) have recently demonstrated that the instantaneous net pressure gradient (TPG_{net}) across the valve during LV ejection, that is, the difference between the LV pressure and the pressure in the ascending aorta (P_A), can be written as:

$$TPG_{net}(t) = P_V(t) - P_A(t) = \frac{2\pi\rho}{\sqrt{E_LCo}} \frac{\partial Q(t)}{\partial t} + \frac{\rho}{2} \frac{Q^2(t)}{E_LCo^2} \quad (2)$$

where ρ is the fluid density, Q is the transvalvular flow rate, and E_LCo is the energy loss coefficient of the aortic valve (12, 13). E_LCo is a function of the valve effective orifice area (EOA) and the aortic

Address for reprint requests and other correspondence: D. Garcia, Biomedical Engineering Laboratory, IRCM, 110 Pine West Ave., Montreal, Quebec, Canada H2W 1R7 (E-mail: Damien.Garcia@ircm.qc.ca).

The costs of publication of this article were defrayed in part by the payment of page charges. The article must therefore be hereby marked “advertisement” in accordance with 18 U.S.C. Section 1734 solely to indicate this fact.

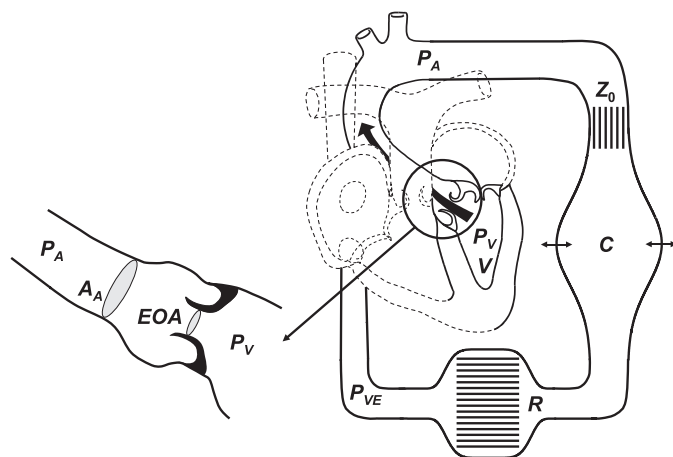


Fig. 1. Schema of the ventricular-valvular-vascular interaction mathematical model. P_V , left ventricular (LV) pressure; V , LV volume; EOA, effective orifice area of the aortic valve; A_A , cross-sectional area of the aorta at the sinotubular junction; P_A , pressure in the ascending aorta; Z_0 , aortic characteristic impedance; C , total arterial compliance; R , systemic vascular resistance; P_{VE} , central venous pressure.

cross-sectional area (A_A) and is defined as $E_LCo = EOA A_A/(A_A - EOA)$. The so-called aortic valve EOA is the minimal cross-sectional area of the flow jet, i.e., the cross-sectional area of the vena contracta, downstream of a native or bioprosthetic aortic heart valve (Fig. 1). Finally, the three-element windkessel model relates the P_A to the transvalvular flow rate (Q) as follows:

$$\frac{\partial P_A(t)}{\partial t} + \frac{P_A(t)}{RC} = \frac{Z_0 + R}{RC} Q(t) + Z_0 \frac{\partial Q(t)}{\partial t} + \frac{P_{VE}}{RC} \quad (3)$$

where Z_0 is the aortic characteristic impedance, R is the total vascular resistance, C is the total arterial compliance, and P_{VE} is the central venous pressure. Figure 1 depicts a schema of the complete coupling model. The sum $\partial(Eq. 2)/\partial t + (Eq. 2)/(RC)$ yields:

$$\frac{\partial(P_V - P_A)}{\partial t} + \frac{(P_V - P_A)}{RC} = \frac{2\pi\rho}{\sqrt{E_LCo}} \left(\frac{\partial^2 Q}{\partial t^2} + \frac{1}{RC} \frac{\partial Q}{\partial t} \right) + \frac{\rho}{2E_LCo^2} Q \left(2 \frac{\partial Q}{\partial t} + \frac{Q}{RC} \right) \quad (4)$$

The second term of Eq. 3 is substituted for the expression $\partial P_A/\partial t + P_A/RC$ in the first term of Eq. 4, and P_V is replaced using Eq. 1. Also, during ejection, transvalvular flow rate can be written as: $Q(t) = -\partial V(t)/\partial t$. Therefore, Eq. 4 becomes:

$$\frac{2\pi\rho}{\sqrt{E_LCo}} \frac{\partial^3 V(t)}{\partial t^3} = a_3(t) \frac{\partial^2 V(t)}{\partial t^2} + a_2(t) \frac{\partial V(t)}{\partial t} + a_1(t)V(t) + a_0(t) \quad (5)$$

where

$$\begin{cases} a_0(t) = V_0 \frac{\partial E(t)}{\partial t} + V_0 \frac{E(t)}{RC} + \frac{P_{VE}}{RC} \\ a_1(t) = -\frac{\partial E(t)}{\partial t} - \frac{E(t)}{RC} \\ a_2(t) = \frac{\rho}{2RC E_LCo^2} \frac{\partial V(t)}{\partial t} - \frac{Z_0 + R}{RC} - E(t) \\ a_3(t) = \frac{\rho}{E_LCo^2} \frac{\partial V(t)}{\partial t} - \frac{2\pi\rho}{RC \sqrt{E_LCo}} - Z_0 \end{cases}$$

At the onset of the ejection ($t = t_0$), V is equal to the LV end-diastolic volume (LVEDV) and $Q = 0$. Ejection begins when LV

pressure reaches aortic pressure, i.e., when TPG_{net} is zero. According to Eq. 2, $\partial Q/\partial t$ is thus also equal to zero at the ejection onset. Because $Q(t) = -\partial V(t)/\partial t$, the initial conditions are therefore:

$$V(t_0) = LVEDV; \quad \frac{\partial V}{\partial t}(t_0) = 0; \quad \frac{\partial^2 V}{\partial t^2}(t_0) = 0 \quad (6)$$

The third-order nonlinear differential Eq. 5 and the corresponding initial conditions (Eq. 6) completely describe the LV volume during ejection in the presence of aortic stenosis under the conditions that the ventricular contractility, the arterial properties, and the aortic stenosis severity are known. The transvalvular flow rate is simply calculated using the negative derivative of $V(t)$. It has been shown that the normalized elastance (E_N) is quasi-independent of the preload, the afterload, and the cardiac inputs (30, 35). Elastance $E(t)$ can thus be defined from its peak value (E_{max}) and time to E_{max} (T_{Emax}) as follows: $E(t) = E_{max} E_N(t/T_{Emax})$ (30). Table 1 summarizes the independent parameters necessary for simulating LV volume during ejection using the V^3 model.

Numerical computation. Time reference ($t = 0$) is fixed at the onset of the isovolumic contraction. The computational algorithm is somewhat equivalent to the one used by Segers et al. (26). An arbitrary diastolic pressure (DP_A) is chosen. Time corresponding to the ejection onset (t_0) is determined from Eq. 1 such that t_0 satisfies the following equation: $E(t_0) = DP_A/(LVEDV - V_0)$. LV volume during ejection is then calculated from Eqs. 5 and 6 using an explicit Runge-Kutta method. The end of LV ejection is reached when $Q(t)$ becomes zero and it is further assumed that $Q = 0$ during diastole. P_A is then deduced using Eq. 3 with the calculated transvalvular flow rate (see APPENDIX). A second DP_A is therefore obtained. If the relative difference between the two DP_A is $>1\%$, a new iteration is performed using the second DP_A value and so on until the desired relative precision is reached. P_V during isovolumic contraction, ejection, and isovolumic relaxation is then calculated from Eq. 1 and is extrapolated during the ventricular filling period using an exponential function (see APPENDIX).

Clinical protocol. Clinical materials and methods are described in detail by Dekker et al. (9). Briefly, LV and aortic pressures, LV volume, and ECG were measured in six symptomatic patients with severe aortic valve stenosis just before and just after the aortic valve replacement. All patients provided their consent, and the study was approved by the institutional committee of the Academic Hospital of Maastricht. LV volume and pressure were obtained by inserting a conductance catheter with a pressure sensor (Sentron ANP-223N, Roden, The Netherlands) into the left ventricle. The conductance catheter was connected to a Leycom Sigma 5DF system (CD Leycom, Zoetermeer, The Netherlands) used in the dual-frequency mode. P_A was measured using a pressure tip catheter (Sentron ANP-530N, Roden, The Netherlands) positioned in the aortic root.

Hemodynamic data (LV and aortic pressures and LV volume) were acquired over a few cardiac cycles before cardiopulmonary bypass when the hemodynamics conditions were stable (dataset 1), and then

Table 1. Cardiovascular parameters needed for the complete resolution of the V^3 model

Ventricular parameters	
Left ventricular end-diastolic volume	LVEDV
Unloaded volume	V_0
Maximal elastance	E_{max}
Time to maximal elastance	T_{Emax}
Vascular parameters	
Aortic characteristic impedance	Z_0
Systemic vascular resistance	R
Total arterial compliance	C
Central venous pressure	P_{VE}
Valvular parameter	
Energy loss coefficient	E_LCo

a series of pressure-volume loops were acquired during inferior caval vein occlusion (*dataset 2*). The same protocol was repeated 15 min after successful weaning from the cardiopulmonary bypass. Pressure-volume loops during caval vein occlusion could not be obtained preoperatively in two patients due to the presence of ectopic beats. The onset of the isovolumic contraction was detected from the peak of the QRS wave of the ECG signal.

Estimation of cardiovascular parameters in patients. For each patient, the normalized elastance was determined before and after valve replacement from the series of pressure-volume loops contained in *dataset 2*. E_{\max} and V_0 were first calculated according to the method described by Kono et al. (16). With V_0 known, elastance was then determined from Eq. 1 for each loop, and the average value was computed and used thereafter. E_N was obtained by dividing elastance by E_{\max} . $T_{E_{\max}}$ was calculated as the elapsed time between the onset of the isovolumic contraction and time when elastance is maximal; i.e., when $E(t) = E_{\max}$. LVEDV was directly obtained from the LV volume waveforms measured during the steady-state condition (*dataset 1*). The other parameters E_{\max} , V_0 , R , C , Z_0 , P_{VE} , and E_{LCo} were estimated using the Nelder-Mead minimization method (17). The function to be minimized was the sum of the relative errors between measured and simulated LV and aortic pressures, respectively. Typical values encountered in the literature were used as initial estimates. We chose to estimate E_{\max} and V_0 with the use of the minimization method rather than to use those calculated from the LV pressure-volume loops of *dataset 2*, because LV contractility may vary significantly during operation (4, 9). Indeed, according to our preliminary calculations, we observed that E_{\max} and V_0 measured during caval vein occlusion were different from those calculated during the steady-state condition. Once the minimization was completed, P_V and P_A and stroke volume (SV) estimated by the model were compared with the averaged experimental data to validate the V^3 model.

Comparison of estimated and measured pressures. Estimated P_V and P_A were compared with measured pressures by calculating the total relative error defined as:

total relative error (%)

$$= 50 \left(\frac{|\text{computed } P_V - \text{measured } P_V|}{|\text{measured } P_V|} + \frac{|\text{computed } P_A - \text{measured } P_A|}{|\text{measured } P_A|} \right)$$

where $|\dots|$ represents the vectorial 1-norm. The goodness of fit was evaluated by performing a linear regression using all the data points from the pressure waveforms, and the coefficient of determination (r^2), as well as the root mean square error, were determined. We also calculated the mean of the residuals, defined as the differences between the measured pressures and the fitted pressures, and we studied their correlation with the measured pressure data to test whether the residuals displayed a systematic pattern. A similar analysis was performed with LV volumes measured and simulated during LV ejection.

Statistical analysis. Standard cardiovascular parameters (heart rate; stroke volume; cardiac output; LV end-diastolic and end-systolic volumes; LV ejection fraction; LV end-diastolic, peak, and end-systolic pressures; aortic systolic, diastolic and mean pressures; mean transvalvular pressure gradient; and Gorlin EOA) were measured for each patient. The data measured before valve replacement were compared with those measured after valve replacement with the use of a two-tailed paired t -test. A similar statistical analysis was also performed with the seven cardiovascular parameters estimated by the minimization method (E_{\max} , V_0 , R , C , Z_0 , P_{VE} , and E_{LCo}).

RESULTS

Normalized elastance before and after aortic valve replacement. Aortic valve replacement did not significantly alter E_N for a given patient, as shown in Fig. 2. Because it was impossible to measure E_N in *patients 3* and *5* before valve replacement and given that the E_N remained unchanged during surgery in all other patients, we chose to use the E_N determined postoperatively to simulate preoperative LV and aortic pressures in these two patients.

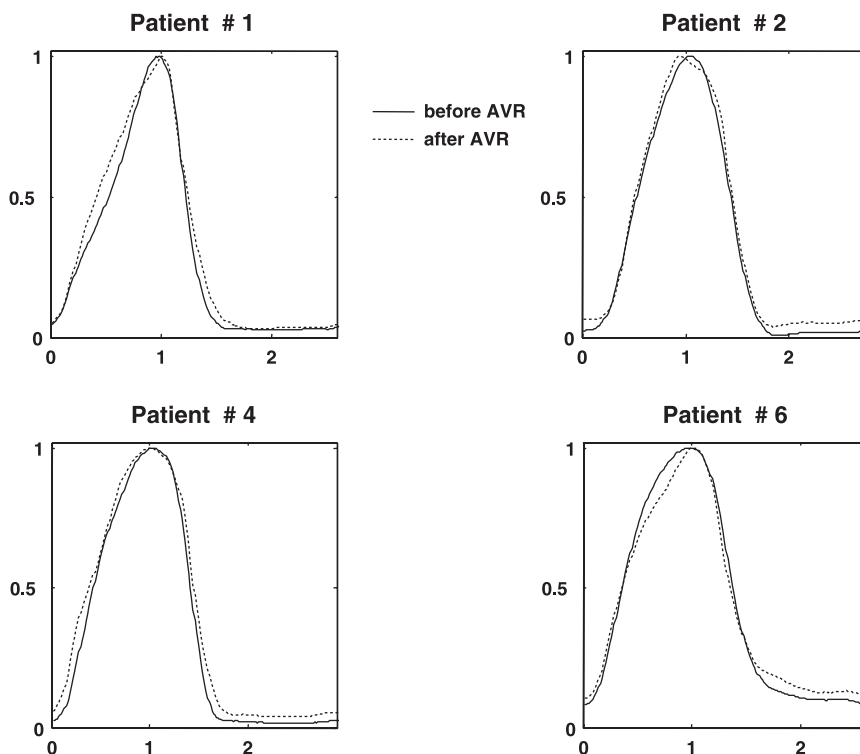


Fig. 2. Normalized elastance before (solid lines) and after (dotted lines) aortic valve replacement (AVR). Comparison is not possible in *patients 3* and *5* because P-V loop data could not be obtained before surgery.

Table 2. Cardiovascular parameters measured before and after valve replacement for the 6 patients

	Before	After	P Value
Heart rate, beats/min	75 (SD 6)	79 (SD 5)	NS
Stroke volume, ml	58 (SD 16)	61 (SD 12)	NS
Cardiac output, l/min	4.4 (SD 1.3)	4.8 (SD 0.88)	NS
LV end-diastolic volume, ml	119 (SD 34)	102 (SD 11)	NS
LV end-systolic volume, ml	61 (SD 21)	41 (SD 11)	<0.05
LV ejection fraction, %	49 (SD 7)	60 (SD 9.5)	NS
LV end-diastolic pressure, mmHg	13 (SD 7)	11 (SD 3)	NS
LV end-systolic pressure, mmHg	83 (SD 12)	77 (SD 17)	NS
LV peak systolic pressure, mmHg	163 (SD 24)	110 (SD 17)	<0.001
Aortic systolic pressure, mmHg	98 (SD 12)	95 (SD 23)	NS
Aortic diastolic pressure, mmHg	60 (SD 10)	56 (SD 14)	NS
Mean aortic pressure, mmHg	72 (SD 10)	72 (SD 17)	NS
Arterial compliance, ml/mmHg	1.55 (SD 0.37)	1.64 (SD 0.42)	NS
Vascular resistance, mmHg·s·ml ⁻¹	1.11 (SD 0.31)	0.91 (SD 0.26)	NS
Gorlin EOA, cm ²	0.59 (SD 0.10)	1.58 (SD 0.52)	<0.004
Mean pressure gradient, mmHg	48 (SD 16)	12 (SD 6)	<0.002

Values in parentheses are standard deviations (SD). LV, left ventricular; EOA, effective orifice area; NS, not significant.

Comparison of cardiovascular parameters before and after aortic valve replacement. The mean values and standard deviation of cardiovascular parameters measured before and after valve replacement are shown in Table 2. Among these parameters, only LV peak systolic pressure, Gorlin EOA, and mean transvalvular pressure gradient were significantly different before versus after valve replacement. Consistently, among the cardiovascular parameters determined from the minimization method, only E_LCo changed significantly after replacement (Table 3). Hence, only valvular characteristics were significantly and markedly improved after valve replacement. There was no significant improvement in the vascular and ventricular parameters (except LV peak systolic pressure) immediately after valve replacement. Nonetheless, the parameters of LV systolic function (LV end-systolic volume, LV ejection fraction, and SV) tended to improve after valve replacement, but the differences did not reach statistical significance, likely because of the small number of patients included in this study. E_{max} decreased in all patients after valve replacement (Table 3). The difference between pre- and postreplacement E_{max} values was not statistically significant ($P = 0.07$) when analyzed with a two-sided paired t -test but reached statistical significance ($P = 0.03$) when analyzed with a one-sided paired t -test. The decrease in E_{max} after valve replacement may be related to the acute depression of myocardial contractility that is commonly observed after cardiopulmonary bypass. In addition, it is also possible that the reduction in LV systolic

pressure resulting from valve replacement may have contributed to the decrease in E_{max} , because it has been suggested that E_{max} is not completely independent of LV afterload (34).

It is also interesting to note that *patient 6* had a relatively high residual transvalvular pressure gradient (28 mmHg) after valve replacement (see Fig. 7). The E_LCo was only 0.75 cm² (see Fig. 10), and the energy loss index (E_LCo indexed for body surface area: 1.98 m² in this patient) was 0.38 cm²/m² after replacement, which is consistent with severe patient-prosthesis mismatch (24) and definitely explains the high gradient in this patient.

Estimated versus measured LV volumes and SV. Overall, there was a very good agreement between estimated and measured LV volume waveforms as shown in Figs. 3 and 4. Total relative error ranged between 1.2% (*patient 4* before surgery, Fig. 3) and 8.9% (*patient 6* after surgery, Fig. 4) and was on average (standard deviation) 5.3% (SD 2.7). Slope and intercept (with 95% confidence interval) of the regression line between estimated and measured volume data during ejection were 0.95 (0.947, 0.955) and 3.84 (3.49, 4.18) ml, respectively, and r^2 was 0.978. The root-mean-square error was 4.4 ml. The mean (SD) of the residuals was 0.00 (SD 4.4) ml, and no correlation was found ($r < 10^{-3}$) between the residuals and the volume data, suggesting that the residuals behaved randomly. These data confirm that there was a good fit between the LV volume waveforms simulated by the V^3 model and those directly measured in patients. Measured LV SV ranged be-

Table 3. Cardiovascular parameters estimated by the minimization method before and after valve replacement in each patient

Patient No.	E_{max} , mmHg/ml		V_0 , ml		R , mmHg·s·ml ⁻¹		C , ml/mmHg		Z_0 , mmHg·s·ml ⁻¹		P_{VE} , mmHg		E_LCo , cm ²	
	Before	After	Before	After	Before	After	Before	After	Before	After	Before	After	Before	After
1	2.6	2.1	4	0	0.96	0.60	1.7	2.4	0.066	0.051	5.3	5.9	0.65	1.5
2	1.1	1.0	-87	-54	1.3	0.57	1.2	2.0	0.078	0.063	4.7	4.8	0.52	1.9
3	4.3	3.1	47	16	1.1	1.2	1.5	1.2	0.076	0.096	6.1	5.0	0.56	1.8
4	3.1	1.4	49	-7	0.81	0.59	1.6	1.7	0.085	0.067	5.2	4.6	0.55	2.0
5	1.4	1.2	-13	-52	0.57	0.94	2.2	1.0	0.047	0.073	5.5	4.3	0.85	1.8
6	2.0	1.9	-29	7	0.67	0.54	1.2	1.6	0.085	0.069	5.6	5.2	0.45	0.75
Mean (SD)	2.4 (1.2)	1.8 (0.8)	-5 (51)	-15 (30)	0.90 (0.27)	0.74 (0.27)	1.6 (0.4)	1.6 (0.5)	0.073 (0.014)	0.070 (0.015)	5.4 (0.5)	5.0 (0.5)	0.60 (0.14)	1.6 (0.5)
P value	NS		NS		NS		NS		NS		NS		<0.002	

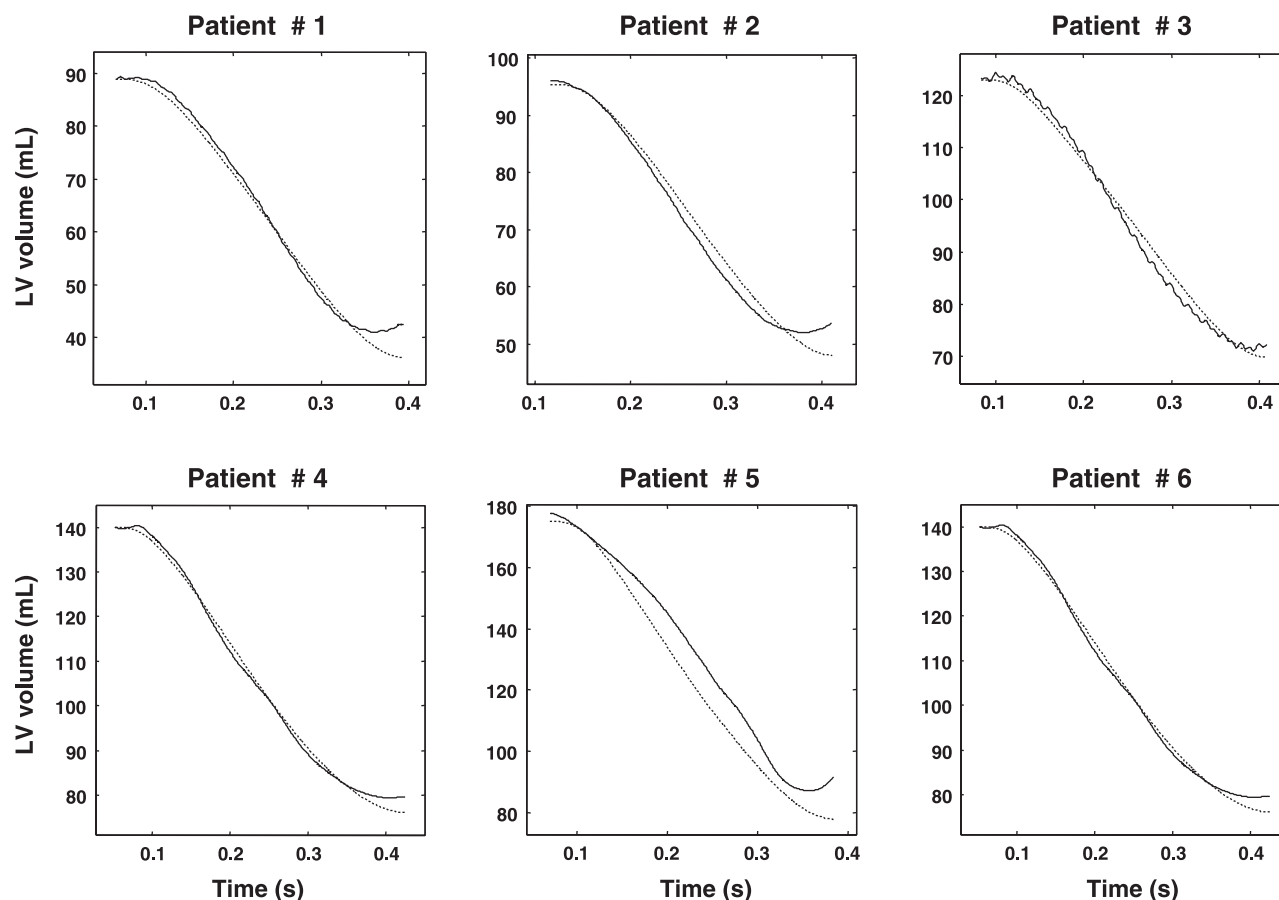


Fig. 3. Comparison between measured (solid lines) and estimated (dotted lines) LV volume waveforms during ejection in the six patients before AVR.

tween 43 and 88 ml. There was an excellent agreement between estimated and measured SV ($y = 1.03x + 2.2$, $r^2 = 0.96$, SEE = 2.8 ml, Fig. 5). The mean (SD) absolute error was 3.8 (SD 2.7) ml.

Estimated versus measured pressure waveforms. Overall, there was a very good agreement between estimated and measured pressure waveforms as shown in Figs. 6 and 7. Total relative error ranged between 3.7% (patient 3 after surgery, Fig. 7) and 10.5% (patient 4 after surgery, Fig. 7) and was on average 7.5% (SD 2.3). Slope and intercept of the regression line between the simulated and the measured pressure data were 0.99 (95% confidence interval: 0.9981, 1.002) and -2.36 (-2.50 , -2.22) mmHg, respectively, and r^2 was 0.98. The root-mean-square error was 6.0 mmHg. The mean (SD) of the residuals was 0.0 (SD 6.0) mmHg, and no correlation was found ($r < 0.001$; P = not significant) between the residuals and the pressure data. These results show that there was an excellent fit between the pressure waveforms generated by the V^3 model and the pressure waveforms directly measured in patients.

Comparison between estimated and measured cardiovascular parameters. In this study, seven among the nine parameters included in the model (Table 1) were estimated by the Nelder-Mead minimization method. The individual and average data of these parameters estimated by minimization are shown in Table 3. The minimization method usually provides a local minimum and not a global minimum of the function to be minimized around the chosen starting point. For a complex

system, such as the one described by the V^3 model, it is uncertain whether there is only one unique set of values for these parameters, which leads to a good concordance between the pressure waveforms. To confirm that the detected local minimum corresponds to the actual value of the cardiovascular parameters, we therefore compared three of these parameters, i.e., R , C , and E_LCo , obtained from the minimization method with those directly obtained from the experimental measurements. R and C were calculated with the equations used in clinical practice and were thus represented by the abbreviations R_{clin} and C_{clin} , respectively:

$$R_{clin} = (MAP - P_{VE})T/SV \quad (7)$$

and

$$C_{clin} = SV/PP \quad (8)$$

where MAP, PP, and T represent the mean aortic pressure, the pulse pressure, and the cardiac period, respectively. We previously demonstrated that E_LCo is equivalent to the valve EOA calculated using the standard Gorlin formula (in cm^2): $EOA_{Gorlin} = Q_{mean}/(44.3 \sqrt{TPG_{net}})$, where Q_{mean} (in ml/s) is the mean transvalvular flow rate and TPG_{net} (in mmHg) is the mean net transvalvular pressure gradient, which includes the pressure recovery occurring downstream of the vena contracta (39). For the purpose of this analysis, E_LCo was thus compared with EOA_{Gorlin} .

As shown in Figs. 8–10, there was a strong correlation between the parameters estimated by the optimization method

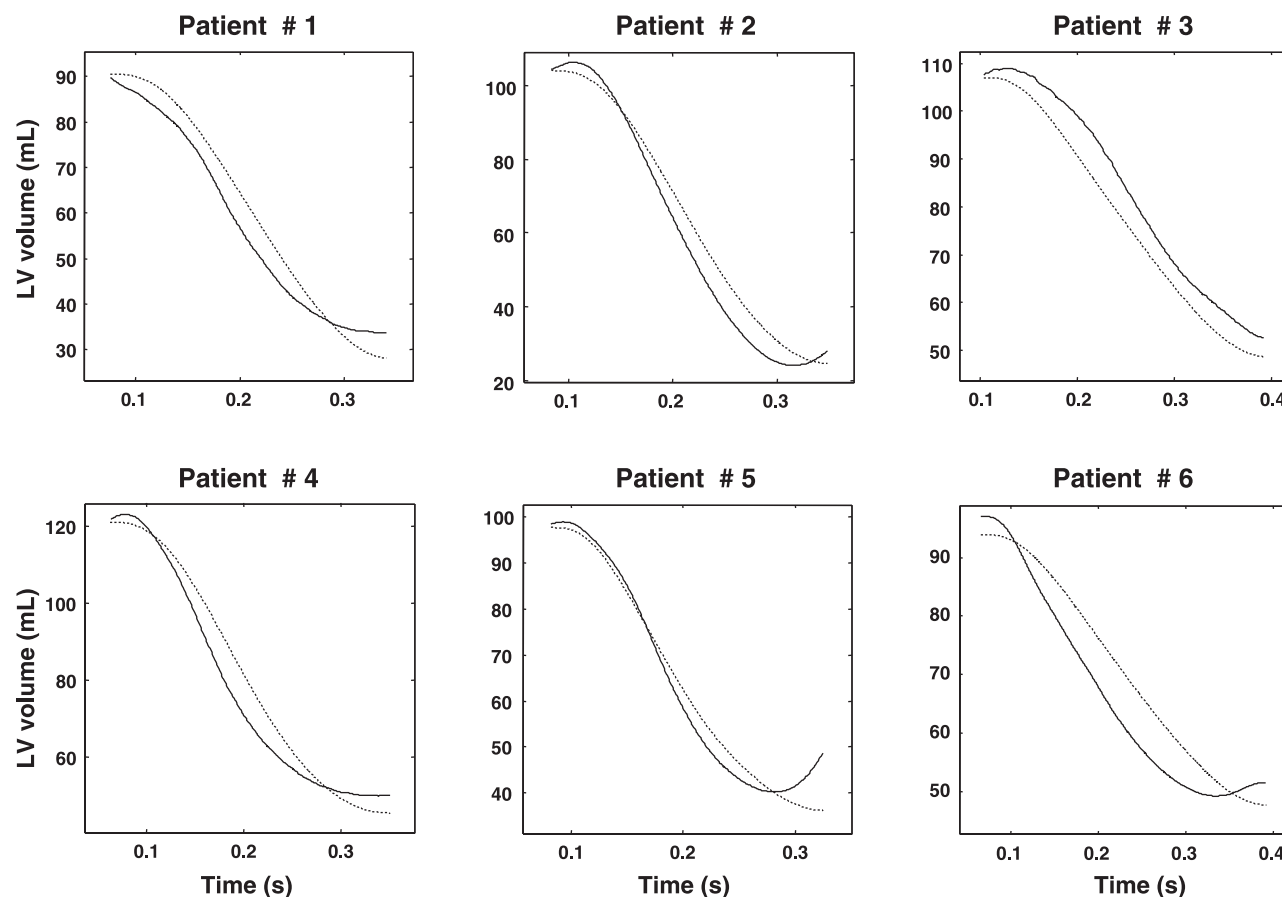


Fig. 4. Comparison between measured (solid lines) and estimated (dotted lines) LV volume waveforms during ejection in the six patients after AVR.

and the parameters obtained from experimental measurements (estimated vs. measured: resistance, $y = 0.91x - 0.04$, $r^2 = 0.98$; compliance, $y = 1.12x - 0.15$, $r^2 = 0.94$; energy loss coefficient, $y = 1.00x + 0.04$, $r^2 = 0.95$). This suggests that

the minimization algorithm likely converges toward a consistent minimum.

DISCUSSION

V^3 model. A few LV-arterial coupling models have been proposed to analyze the effect of vascular properties on LV function (10, 27, 32, 36, 41). The model proposed by Segers et al. (26, 32) is relatively simple and easily applicable in the clinical setting. This model accurately predicted the SV and the systolic and diastolic aortic pressures in animals and in humans. The model of Segers et al. (26, 32) is based on the combination of the time-varying elastance representation of the left ventricle with a four-element windkessel model. However, this model assumes that the aortic valve is normal and it is thus not applicable in patients with an aortic stenosis. Computer models also including the effect of aortic stenosis have been proposed by Li et al. (18) and Smith et al. (31). In these models, the aortic stenosis was represented by the valve resistance defined by the Ohm's law as the ratio of TPG to Q. However, other investigators (2, 5, 37) have demonstrated that the resistance is not appropriate to describe the LV burden imposed by the stenotic valve. In the present study, we utilized the model proposed by Segers et al. in which we incorporated an analytic model of the transvalvular pressure gradient. This mathematical model of aortic stenosis is based on the energy loss concept as described by Eq. 2, and it has been recently

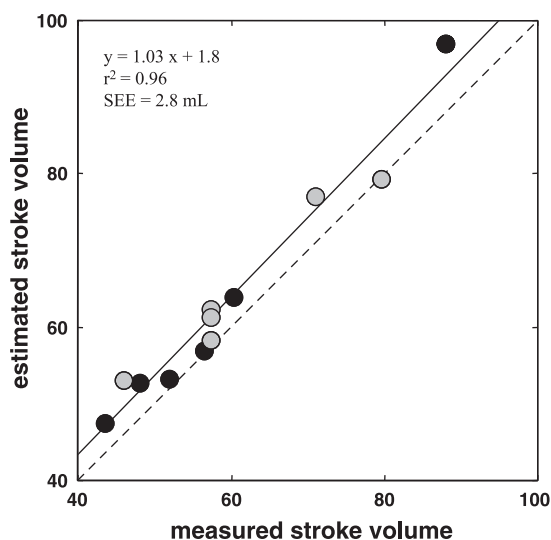


Fig. 5. Relationship between measured stroke volume (in ml) and that estimated from the minimization method. Dotted line, identity line. Black and grey dots correspond to data before and after surgery, respectively.

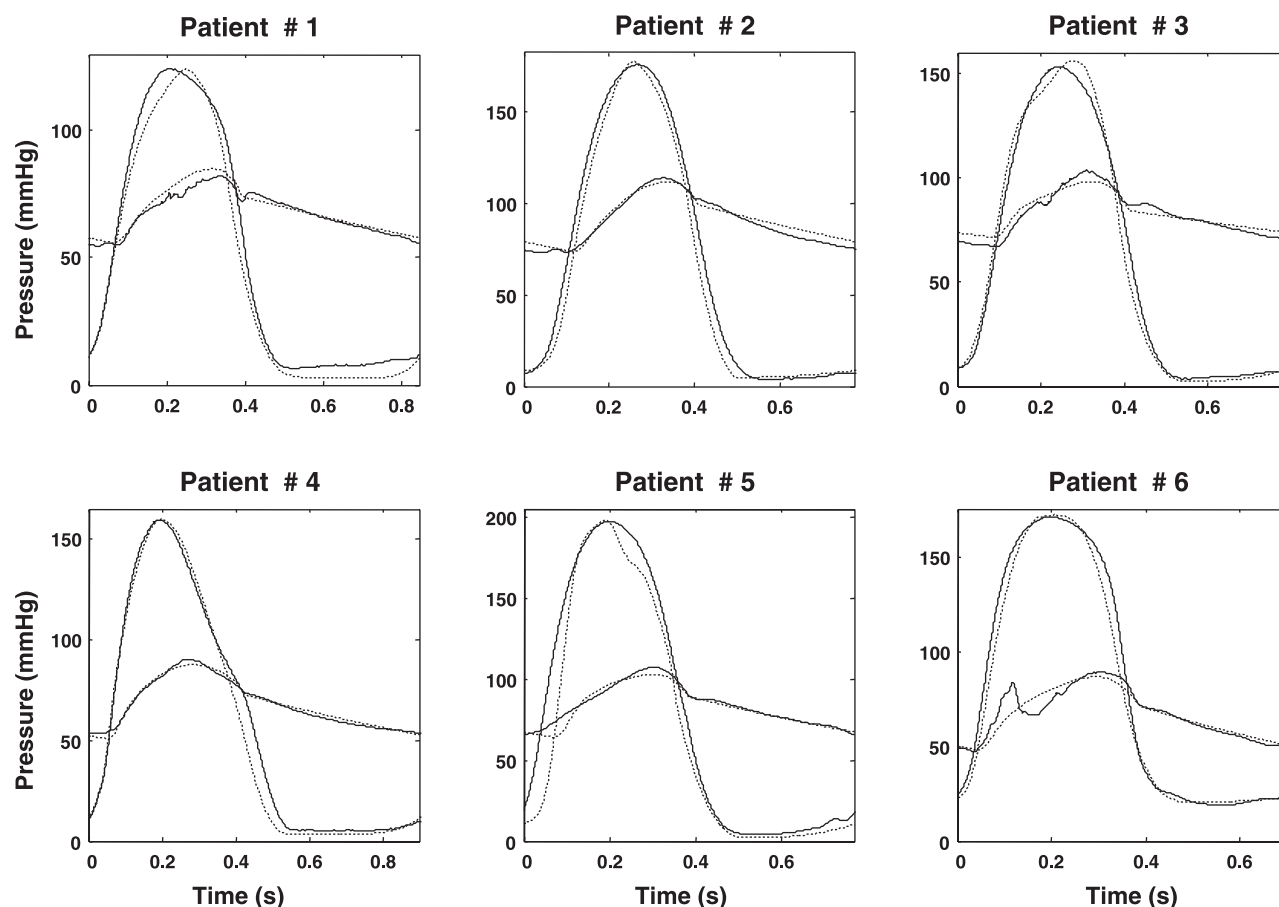


Fig. 6. Comparison between measured (solid lines) and estimated (dotted lines) LV and aortic pressure waveforms in the six patients before AVR.

validated in vitro (13). The resulting V^3 model is thus represented by a third-order nonlinear differential equation whose resolution can be performed using appropriate initial conditions (see Eqs. 5 and 6). The main advantage of the V^3 model is that it may explicitly and accurately describe the behavior of LV volume during ejection if a few (nine) cardiovascular parameters are known.

LV normalized elastance. The LV elastance normalized with respect to its amplitude and time to peak value is an essential element of the V^3 model. Although normalized elastance was similar before and after aortic valve replacement in a given patient, it was different from one patient to the other (Fig. 2). When every patient is considered, the mean absolute difference between the individual normalized elastances and the averaged normalized elastance was 0.053 (maximum = 0.372). The interindividual variability observed in the present study was higher than that reported in the study of Senzaki et al. (30). In their study that included 52 patients, the variability of normalized elastance was minimal despite the presence of interindividual differences with regard to etiology of heart disease, LV myocardial contractility, and loading conditions. However, their study did not include patients with aortic stenosis. Moreover, their results are also in disagreement with those recently published by Kjørstad et al. (15), where a considerable variability of the normalized elastance was observed among the patients. Further studies in a larger number of patients with aortic stenosis are thus needed to assess the interindividual variability of normalized elastance in these patients.

Cardiovascular parameters. As expected, the systemic vascular resistance estimated by the minimization method was systematically lower than that calculated from experimental data (Fig. 8). Indeed, it can be shown from Eqs. 3 and 7 that R_{clin} is related to R as follows: $R_{\text{clin}} = R + Z_0$. The aortic characteristic impedance was not measured in the present study. Nonetheless, the value estimated by the minimization method ($0.071 \pm 0.014 \text{ mmHg} \cdot \text{s} \cdot \text{ml}^{-1}$) was very consistent with that observed in patients by other investigators (19).

Although Segers et al. (29) reported in an animal study that the stroke volume-to-aortic pulse pressure ratio (Eq. 8) systematically underestimates the compliance determined by the area method, Chemla et al. (7) showed that it provides an accurate estimation of the total arterial compliance in patients with a normal aortic valve. Our results (Fig. 9) are consistent with the results of Chemla et al., and they suggest that the stroke volume-to-aortic pulse pressure ratio may also be valid to estimate compliance in patients with aortic stenosis as well as in patients with aortic valve prosthesis. This observation, however, remains to be confirmed in a larger number of patients with aortic stenosis.

Garcia et al. (11) demonstrated that there is a strong agreement between the E_{LCo} and the EOA determined by the Gorlin formula in animals with experimentally induced supravalvular aortic stenosis as well as in patients with aortic valve stenosis. They also showed that E_{LCo} and $\text{EOA}_{\text{Gorlin}}$ are equivalent parameters that accurately reflect the energy loss caused by the

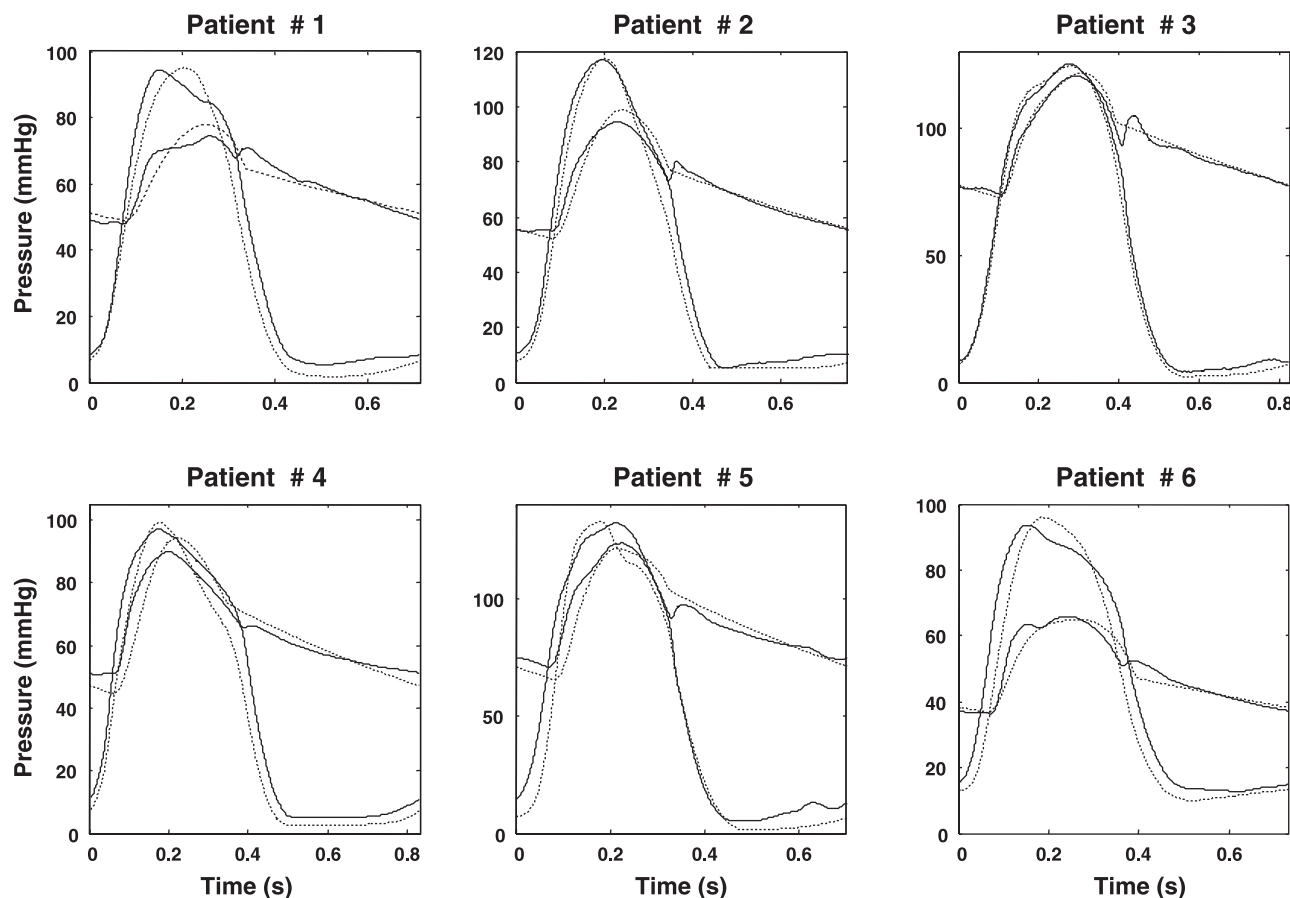


Fig. 7. Comparison between measured (solid lines) and estimated (dotted lines) LV and aortic pressure waveforms in the six patients after AVR.

valvular stenosis. The good concordance between the E_LCo estimated by the minimization method in the present study and the EOA determined by the Gorlin formula (Fig. 10) is consistent with these previous results.

Limitations of the mathematical model. In the V^3 model, we chose a three-element windkessel model even though it has been recently shown by Stergiopoulos et al. (33) that a four-element model, including the so-called arterial inertance, is

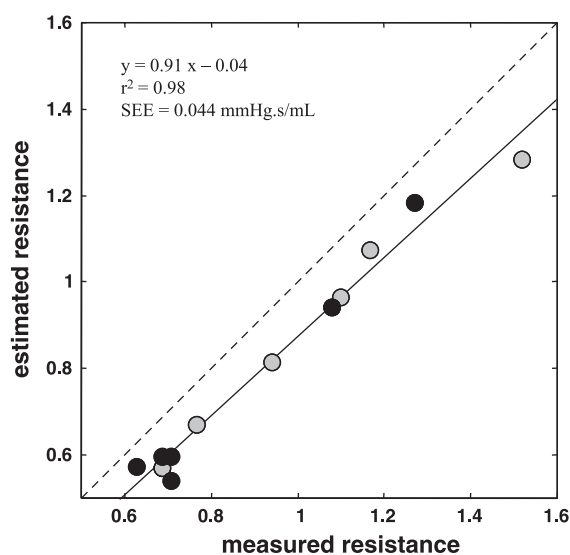


Fig. 8. Relationship between resistance (in $\text{mmHg} \cdot \text{s} \cdot \text{ml}^{-1}$) measured using the standard clinical formula (Eq. 7) and that estimated from the minimization method. Dotted line, identity line. Solid and shaded circles correspond to data before and after surgery, respectively.

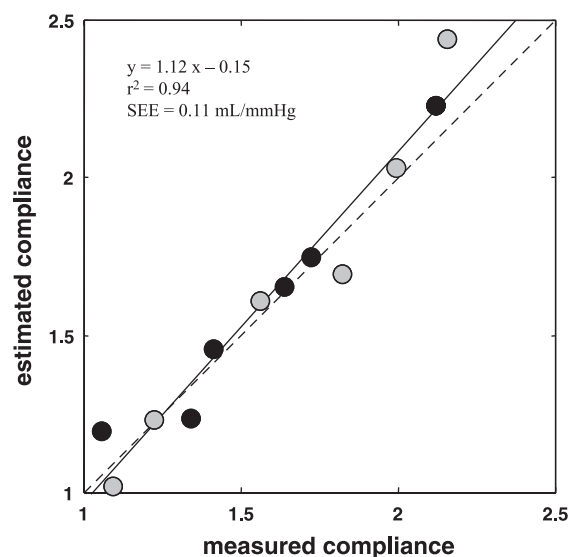


Fig. 9. Relationship between compliance (in ml/mmHg) measured using the standard clinical formula (Eq. 8) and that estimated from the minimization method. Dotted line, identity line. Solid and shaded circles correspond to data before and after surgery, respectively.

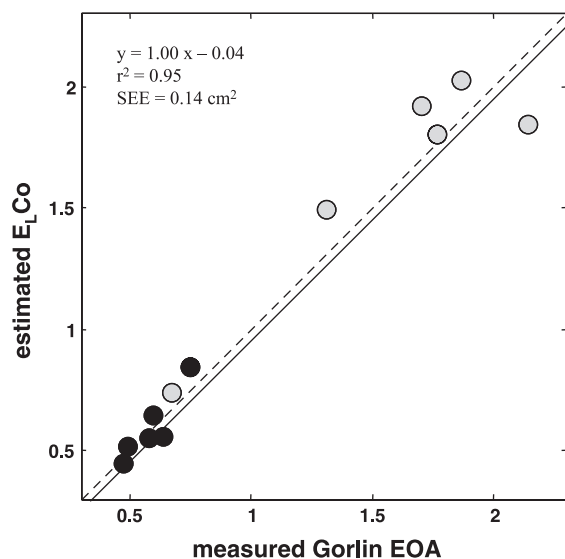


Fig. 10. Comparison between EOA (in cm^2) measured using the Gorlin formula and energy loss coefficient (E_LCo) estimated from the minimization method. Dotted line, identity line. Solid and shaded circles correspond to data before and after surgery, respectively. Note the severe patient-prosthesis mismatch in patient 6 (isolated gray circle).

superior in describing the vascular properties. Inserting this fourth element in our coupling model would have resulted in a fourth-order differential equation for the LV volume, which would have therefore necessitated an additional initial condition (see Eq. 6), which is a priori unavailable. This would have therefore resulted in an implicit coupling model that is difficult to apply in the clinical situation. On the other hand, the utilization of the three-element windkessel model provided an explicit model of the LV volume during ejection, which is easily applicable in the context of clinical studies. According to our results, this simplification of our model was not a major limitation, because the estimated compliance and resistance were very consistent with the ones directly obtained from experimental data.

The estimated unloaded volume (V_0) was ≤ 0 in seven among the twelve datasets (Table 3). This parameter was estimated by the linear approximation of the pressure-volume relation given by Eq. 1. However, the pressure-volume relationship is not linear when LV volume becomes small (14, 21). Hence, V_0 has no physical or physiological meaning but is rather a virtual parameter computed by extrapolation. Despite this limitation, the time-varying elastance model remains one of the best simple models of the left ventricle dynamics, and its linear characteristic is appropriate over a large physiological range (14).

Potential clinical implications. It is often difficult to perform a comprehensive analysis of the interaction between different physiological systems in the context of a clinical study. Indeed, this approach usually requires the realization of a large number of physiological measurements in a large cohort of patients, and these measurements are often difficult or even impossible to perform in patients. The utilization of mathematical models may overcome this problem. Hence, the V^3 model validated in the present study may be useful to investigate the interaction between the systemic arterial system, the aortic valve, and the left ventricle in different types of cardiovascular diseases.

Moreover, as opposed to other descriptive models previously reported in the literature, the V^3 model should be potentially applicable in the clinical setting.

Several recent studies suggested that the so-called degenerative aortic stenosis is probably due to an atherosclerotic process (22). Hence, in the vast majority of the patients, aortic stenosis is probably not a disease solely limited to the valve but rather one manifestation of an atherosclerotic process involving various components of the vascular system including the aorta. Accordingly, Briand et al. (3) have recently reported that 41% of the patients with aortic stenosis concomitantly have an abnormally low systemic arterial compliance. In addition, previous studies (1, 23) have reported that systemic hypertension is a frequent occurrence (30–40%) in patients with aortic stenosis. These findings underline that patients with aortic stenosis often have abnormal vascular properties. In such patients, the V^3 model may be useful to better assess the respective contributions of the aortic valve and the systemic arterial system to the LV workload in patients having concomitantly aortic stenosis and vascular diseases (i.e., hypertension, atherosclerosis). This could contribute to determine whether the treatment should be targeted on the reduction of the valvular load by aortic valve replacement, on the reduction of the arterial load by medical treatment, or on both aspects. And in this context, the V^3 model may be superior to existing simple methods for characterizing the two components of the LV load. For example, the transvalvular pressure gradient and systolic arterial pressure are often used to assess the magnitude of the valvular and vascular loads, respectively. However, these parameters are highly flow dependent and are therefore subject to pseudonormalization in patients with reduced cardiac output (3). This implies that, in such patients, these parameters may underestimate the impact of the aortic valve and/or of the systemic arterial system on the LV workload. The utilization of parameters that are less flow dependent such as the Gorlin EOA or the E_LCo for the characterization of valvular properties and the arterial resistance and compliance for the characterization of vascular properties may improve the ability to assess the two components of the LV load. However, when these parameters are analyzed separately, it is difficult to estimate what is the independent contribution of each parameter to the overall LV workload. The most frequently used approach to overcome this limitation in clinical studies is to perform multivariate regression analysis. However, this approach assumes a linear relationship between the different parameters, which is obviously not the case in the ventricular-valvular-vascular system. The utilization of a mathematical model such as the V^3 model that relates the aforementioned vascular and valvular parameters with an appropriate formulation may be superior to conventional approaches for the assessment of the respective contributions of the aortic valve and systemic arterial system to the LV workload. This potential clinical usefulness of the V^3 model, however, remains to be confirmed in a larger cohort of patients.

APPENDIX

Determination of aortic pressure. We note t_0 as the time at which ejection begins and T as the cardiac period. The solution of Eq. 3 gives the aortic pressure:

$$P_A(t) = e^{-(t-t_0)/RC} \left(\int_{t_0}^t \frac{Q^*(\tau)}{C e^{-\tau/RC}} d\tau + DP_A - P_{VE} \right) + P_{VE}$$

where Q^* is related to Q as follows:

$$Q^*(\tau) = \frac{Z_0 + R}{R} Q(\tau) + Z_0 C \frac{\partial Q(\tau)}{\partial \tau} + \frac{P_{VE}}{R}$$

and the diastolic aortic blood pressure is found using the periodic property of aortic pressure:

$$DP_A = P_{VE} + \int_{t_0}^{t_0+T} \frac{Q^*(t) e^{(t-t_0)/RC}}{C e^{T/RC} - C} dt$$

Ventricular pressure during the ventricular filling period. Ventricular pressure during the ventricular filling period is extrapolated using the following expression:

$$P_V(t) = a(t - t^*)^n + P_V(t^*)$$

where time t^* corresponds to the end of the isovolumic relaxation. In our study, according to the results of Senzaki et al. (30), we postulated that $t^* = 1.8T_{Emax}$. Parameters a and n were calculated such that P_V is continuously differentiable. Reminding that time reference ($t = 0$) is fixed at the onset of the isovolumic contraction, it can be demonstrated that parameters a and n are thus given by:

$$a = \frac{P_V(0) - P_V(t^*)}{(T - t^*)^n} \quad \text{and} \quad n = \frac{T - t^*}{P_V(0) - P_V(t^*)} \frac{\partial P}{\partial t} \Big|_{t=t^*}$$

REFERENCES

- Antonini-Canterin F, Huang G, Cervesato E, Faggiano P, Pavan D, Piazza R, and Nicolosi GL. Symptomatic aortic stenosis: does systemic hypertension play an additional role? *Hypertension* 41: 1268–1272, 2003.
- Blais C, Pibarot P, Dumesnil JG, Garcia D, Chen D, and Durand LG. Comparison of valve resistance with effective orifice area regarding flow dependence. *Am J Cardiol* 88: 45–52, 2001.
- Briand M, Dumesnil JG, Kadem L, Tongue AG, Rieu R, Garcia D, and Pibarot P. Reduced systemic arterial compliance impacts significantly on LV afterload and function in aortic stenosis: implications for diagnosis and treatment. *J Am Coll Cardiol*. In press.
- Brookes CI, White PA, Bishop AJ, Oldershaw PJ, Redington AN, and Moat NE. Validation of a new intraoperative technique to evaluate load-independent indices of right ventricular performance in patients undergoing cardiac operations. *J Thorac Cardiovasc Surg* 116: 468–476, 1998.
- Burwash IG, Hay KM, and Chan KL. Hemodynamic stability of valve area, valve resistance, and stroke work loss in aortic stenosis: a comparative analysis. *J Am Soc Echocardiogr* 15: 814–822, 2002.
- Chan KL. Is aortic stenosis a preventable disease? *J Am Coll Cardiol* 42: 593–599, 2003.
- Chemla D, Hebert JL, Coirault C, Zamani K, Suard I, Colin P, and Lecarpentier Y. Total arterial compliance estimated by stroke volume-to-aortic pulse pressure ratio in humans. *Am J Physiol Heart Circ Physiol* 274: H500–H505, 1998.
- Cohn JN. Arterial compliance to stratify cardiovascular risk: more precision in therapeutic decision making. *Am J Hypertens* 14: 258S–263S, 2001.
- Dekker AL, Barenbrug PJ, van der Veen FH, Roekaerts P, Mochtar B, and Maessen JG. Pressure-volume loops in patients with aortic stenosis. *J Heart Valve Dis* 12: 325–332, 2003.
- Fitchett DH. LV-arterial coupling: interactive model to predict effect of wave reflections on LV energetics. *Am J Physiol Heart Circ Physiol* 261: H1026–H1033, 1991.
- Garcia D, Dumesnil JG, Durand LG, Kadem L, and Pibarot P. Discrepancies between catheter and Doppler estimates of valve effective orifice area can be predicted from the pressure recovery phenomenon: practical implications with regard to quantification of aortic stenosis severity. *J Am Coll Cardiol* 41: 435–442, 2003.
- Garcia D, Pibarot P, Dumesnil JG, Sakr F, and Durand LG. Assessment of aortic valve stenosis severity: a new index based on the energy loss concept. *Circulation* 101: 765–771, 2000.
- Garcia D, Pibarot P, and Durand LG. Analytical modeling of the instantaneous pressure gradient across the aortic valve. *J Biomech* doi: 10.1016/j.jbiomech.2004.06.018. 2005.
- Kass DA and Maughan WL. From “Emax” to pressure-volume relations: a broader view. *Circulation* 77: 1203–1212, 1988.
- Kjorstad KE, Korvald C, and Myrmet T. Pressure-volume-based single-beat estimations cannot predict left ventricular contractility in vivo. *Am J Physiol Heart Circ Physiol* 282: H1739–H1750, 2002.
- Kono A, Maughan WL, Sunagawa K, Hamilton K, Sagawa K, and Weisfeldt ML. The use of left ventricular end-ejection pressure and peak pressure in the estimation of the end-systolic pressure-volume relationship. *Circulation* 70: 1057–1065, 1984.
- Lagarias J, Reeds J, Wright M, and Wright P. Convergence properties of the Nelder-Mead simplex method in low dimensions. *SIAM J Optimiz* 9: 112–147, 1998.
- Li JK, Zhu JY, and Nanna M. Computer modeling of the effects of aortic valve stenosis and arterial system afterload on left ventricular hypertrophy. *Comput Biol Med* 27: 477–485, 1997.
- Merillon JP, Fontenier GJ, Lerallut JF, Jaffrin MY, Motte GA, Genain CP, and Gourgon RR. Aortic input impedance in normal man and arterial hypertension: its modification during changes in aortic pressure. *Cardiovasc Res* 16: 646–656, 1982.
- Nishimura RA. Cardiology patient pages. Aortic valve disease. *Circulation* 106: 770–772, 2002.
- Noda T, Cheng CP, De Tombe PP, and Little WC. Curvilinearity of LV end-systolic pressure-volume and dP/dt_{max} -end-diastolic volume relations. *Am J Physiol Heart Circ Physiol* 265: H910–H917, 1993.
- Novaro GM and Griffin BP. Calcific aortic stenosis: another face of atherosclerosis? *Cleve Clin J Med* 70: 471–477, 2003.
- Pate GE. Association between aortic stenosis and hypertension. *J Heart Valve Dis* 11: 612–614, 2002.
- Pibarot P and Dumesnil JG. Hemodynamic and clinical impact of prosthesis-patient mismatch in the aortic valve position and its prevention. *J Am Coll Cardiol* 36: 1131–1141, 2000.
- Rossebo AB and Pedersen TR. Hyperlipidaemia and aortic valve disease. *Curr Opin Lipidol* 15: 447–451, 2004.
- Segers P, Steendijk P, Stergiopulos N, and Westerhof N. Predicting systolic and diastolic aortic blood pressure and stroke volume in the intact sheep. *J Biomech* 34: 41–50, 2001.
- Segers P, Stergiopulos N, and Westerhof N. Quantification of the contribution of cardiac and arterial remodeling to hypertension. *Hypertension* 36: 760–765, 2000.
- Segers P, Stergiopulos N, and Westerhof N. Relation of effective arterial elastance to arterial system properties. *Am J Physiol Heart Circ Physiol* 282: H1041–H1046, 2002.
- Segers P, Verdonck P, Deryck Y, Brimiouille S, Naeije R, Carlier S, and Stergiopulos N. Pulse pressure method and the area method for the estimation of total arterial compliance in dogs: sensitivity to wave reflection intensity. *Ann Biomed Eng* 27: 480–485, 1999.
- Senzaki H, Chen CH, and Kass DA. Single-beat estimation of end-systolic pressure-volume relation in humans. A new method with the potential for noninvasive application. *Circulation* 94: 2497–2506, 1996.
- Smith BW, Chase JG, Nokes RI, Shaw GM, and Wake G. Minimal haemodynamic system model including ventricular interaction and valve dynamics. *Med Eng Phys* 26: 131–139, 2004.
- Stergiopulos N, Meister JJ, and Westerhof N. Determinants of stroke volume and systolic and diastolic aortic pressure. *Am J Physiol Heart Circ Physiol* 270: H2050–H2059, 1996.
- Stergiopulos N, Westerhof BE, and Westerhof N. Total arterial inductance as the fourth element of the windkessel model. *Am J Physiol Heart Circ Physiol* 276: H81–H88, 1999.
- Suga H. Cardiac energetics: from E_{max} to pressure-volume area. *Clin Exp Pharmacol Physiol* 30: 580–585, 2003.
- Suga H, Sagawa K, and Shoukas AA. Load independence of the instantaneous pressure-volume ratio of the canine left ventricle and effects of epinephrine and heart rate on the ratio. *Circ Res* 32: 314–322, 1973.
- Ursino M. Interaction between carotid baroregulation and the pulsating heart: a mathematical model. *Am J Physiol Heart Circ Physiol* 275: H1733–H1747, 1998.
- Voelker W, Reul H, Nienhaus G, Stelzer T, Schmitz B, Steegers A, and Karsch KR. Comparison of valvular resistance, stroke work loss, and



- Gorlin valve area for quantification of aortic stenosis. An in vitro study in a pulsatile aortic flow model. *Circulation* 91: 1196–1204, 1995.
38. **Westerhof N, Elzinga G, and Sipkema P.** An artificial arterial system for pumping hearts. *J Appl Physiol* 31: 776–781, 1971.
39. **Wilkinson JL.** Haemodynamic calculations in the catheter laboratory. *Heart* 85: 113–120, 2001.
40. **Willens HJ, Davis W, Herrington DM, Wade K, Kesler K, Mallon S, Brown WV, Reiber JH, and Raines JK.** Relationship of peripheral arterial compliance and standard cardiovascular risk factors. *Vasc Endovascular Surg* 37: 197–206, 2003.
41. **Zacek M and Krause E.** Numerical simulation of the blood flow in the human cardiovascular system. *J Biomech* 29: 13–20, 1996.

